

Temperature Sensitivity of a Two-Mode Photonic Crystal Fiber Interferometric Sensor

Jian Ju, Zhi Wang, Wei Jin, and M. S. Demokan

Abstract—The temperature sensitivity of a two-mode (TM) photonic crystal fiber (PCF) interferometric sensor was investigated theoretically and experimentally. In contrast to the conventional elliptical core TM fiber interferometric sensors, the temperature sensitivity of the PCF sensor has a nonmonotonic dependence on the operating wavelength, and was measured to be 0.083, 0.147, and 0.136 rad/°C · m at 543, 975, and 1310 nm, respectively.

Index Terms—Optical fiber sensor, photonic crystal fiber (PCF), temperature sensitivity, two-mode (TM) fiber.

I. INTRODUCTION

TWO-MODE (TM) optical fibers have found numerous applications in optical fiber sensing and optical fiber devices. Strain and temperature sensors [1], acousto-optic frequency shifters [2], tunable filters [3], and an add-drop multiplexer [4] have been demonstrated on conventional circular and elliptical core TM fibers. In recent years, there has been an increasing interest in photonic crystal fiber (PCF), which consists of a silica core surrounded by a periodic lattice of air holes running along its length. Due to the high flexibility in the fabrication process, PCF can achieve birefringence an order of magnitude higher than conventional highly birefringent (HB) fibers. The HB PCFs fabricated to date are based on different air-hole diameters along two orthogonal axes [5], [6] or on an asymmetric core [7]. We recently found that HB PCF with appropriate structural parameters support only two modes, i.e., LP₀₁ and LP₁₁ (even), over an extremely broad wavelength range of from 500 to 2000 nm [8], [9]. The modal intensity patterns and polarization principal axes are well defined and do not vary along the fiber length or with environmental disturbance. These characteristics coupled with the unique properties of PCF are ideal for the realization of stable TM interferometers over a broad wavelength range. TM PCFs with various structural parameters have been used to construct tunable interferometric optical comb filters [10] and polarimetric sensors for hydrostatic pressure and strain measurement [11]. We have previously investigated the sensitivity of a TM PCF interferometric sensor to longitudinal strain [9]. In this letter, we report the results of our recent investigations on the temperature sensing characteristics of such a TM PCF interferometric sensor.

Manuscript received May 30, 2006; revised August 4, 2006. This work was supported by a grant from the Research Grants Council of the Hong Kong Special Administrative Region, China, under Project PolyU5176/05E.

The authors are with the Department of Electrical Engineering, The Hong Kong Polytechnic University, Hung Hom, Kowloon, Hong Kong (e-mail: eeju@polyu.edu.hk).

Digital Object Identifier 10.1109/LPT.2006.883889

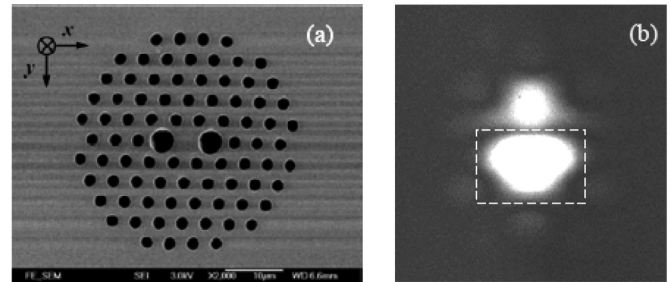


Fig. 1. (a) SEM micrograph of the HB PCF; (b) far-field intensity profile (at 1310 nm) of the TM interferometer output.

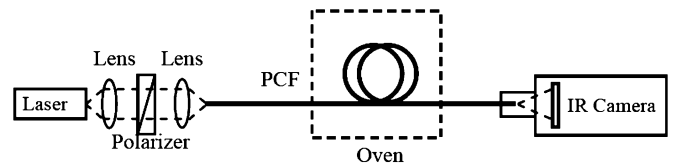


Fig. 2. Experimental setup.

II. MEASUREMENT OF TEMPERATURE SENSITIVITY

The HB PCF used in this work (Fig. 1) is the same as that in [9] and is manufactured by Blaze Photonics. The fiber parameters as determined from the scanning electron micrograph (SEM) are as follows: pitch $\Lambda = 4.179 \mu\text{m}$, diameters of small holes $d_1 = 2.239 \mu\text{m}$, and diameters of larger holes $d_2 = 4.069 \mu\text{m}$. This PCF was previously tested to support two spatial modes, i.e., LP₀₁ and LP₁₁ (even) from 650 nm to 1.3 μm [9]. In the present work, we found the TM range can extend to an even shorter wavelength of 543 nm. At wavelength 1550 nm, the HB PCF supports only the fundamental mode with two orthogonal polarizations. The experimental setup used for measuring the temperature sensitivity is shown in Fig. 2. A polarizer is placed at the input, which allows for the launching of a linear polarization to one of the principal axes of the PCF. A section of PCF (~ 1.8 m) was heated by putting it inside an oven. An infrared camera with lens removed is placed at the output to monitor the far-field intensity distribution. Fig. 1(b) shows one of the recorded far-field intensity distribution when the two modes were excited approximately equally by an offset introduced at the input. The output of the TM interferometer is taken as the average intensity over one of the lobes, i.e., the rectangular area as shown in Fig. 1(b).

Measurements were performed for both the x -polarization and y -polarization. Fig. 3 shows the output intensity (x -polarization) of the TM interferometer as a function of oven temperature. One complete cycle in the intensity variation corresponds to a 2π change in the phase difference between the LP₀₁

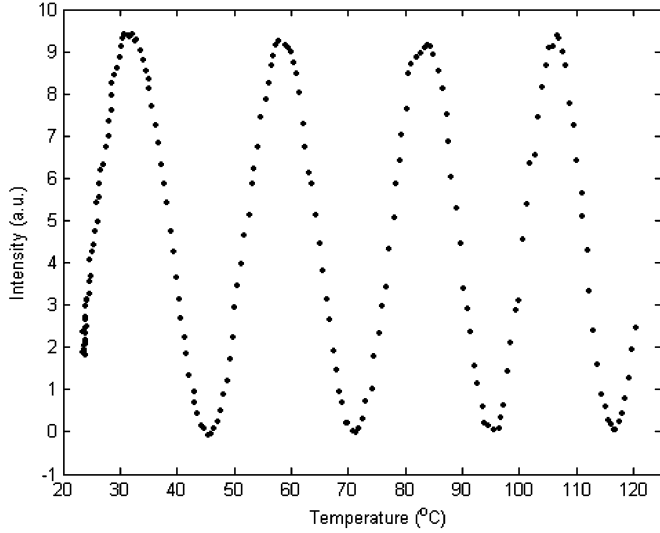


Fig. 3. Experimental results showing the periodic intensity variation with temperature ($\lambda = 1310$ nm, x -polarization).

TABLE I
TEMPERATURE SENSITIVITY (rad/°C · m)

	$\lambda = 543$ nm	$\lambda = 975$ nm	$\lambda = 1310$ nm
x -polarization:	0.083	0.147	0.136
y -polarization:	0.085	0.151	0.145

and LP₁₁ (even) modes. The temperature sensitivity η , defined as the rate of change of phase difference $\Delta\phi$ between the two modes with respect to temperature T per unit length of sensing fiber, is given by

$$\eta = \frac{1}{L} \cdot \frac{\Delta\phi}{\Delta T} \quad (1)$$

where L is the fiber length placed inside the oven. The measured temperature sensitivities are listed in Table I. As can be seen from Table I, the temperature sensitivity of TM PCF is slightly different for the x - and y -polarization. And the values are in general smaller than that of the conventional elliptical core TM fibers [1].

III. THEORETICAL TEMPERATURE SENSITIVITY

The temperature sensitivity η may be rewritten as

$$\eta = \frac{1}{L} \frac{\Delta\phi}{\Delta T} = \frac{1}{L} \cdot \frac{\partial(\Delta\beta \cdot L)}{\partial T} = \frac{\partial(\Delta\beta)}{\partial T} + \Delta\beta \cdot \frac{1}{L} \frac{\partial L}{\partial T} \quad (2)$$

where $\Delta\beta$ is the propagation constant difference between the LP₀₁ and LP₁₁ (even) modes. As the PCF is a single material fiber, the thermal expansion coefficient α and thermooptic coefficient κ should be the same for both the core and cladding, which are respectively defined as

$$\alpha = \frac{1}{L} \cdot \frac{\partial L}{\partial T} \quad \text{and} \quad \kappa = \frac{1}{n} \cdot \frac{\partial n}{\partial T} \quad (3)$$

where n is the refractive index of PCF material. For fused silica, the thermal expansion coefficient and thermooptic coefficient are $\alpha = 5 \cdot 10^{-7}/^\circ\text{C}$ and $\kappa = 1 \cdot 10^{-5}/^\circ\text{C}$, respectively [1].

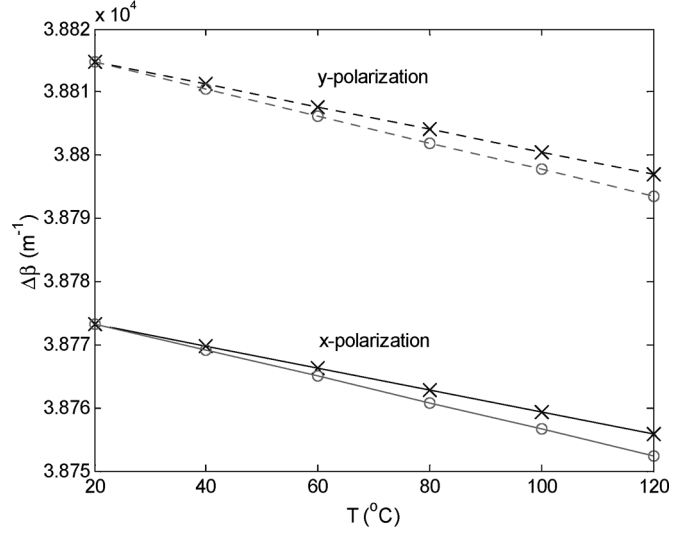


Fig. 4. Propagation constant difference $\Delta\beta$ at 1310 nm as a function of temperature. Circle and cross lines represent the results with and without considering transverse thermal expansion.

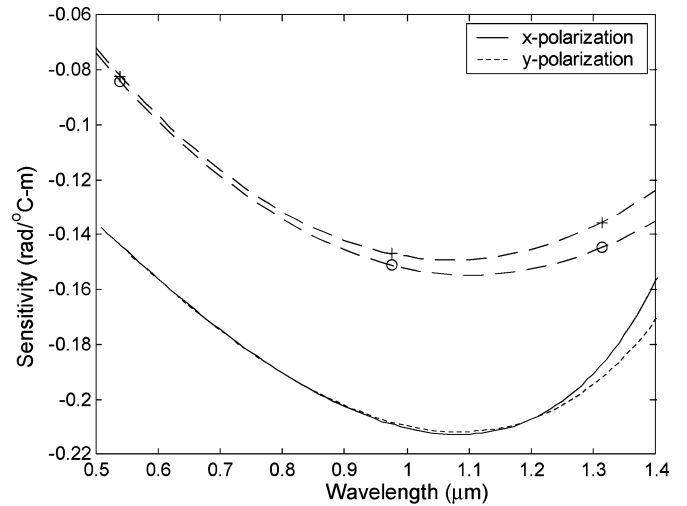


Fig. 5. Calculated temperature sensitivities as functions of wavelength. Solid and dotted lines correspond to theoretical results for the x - and y -polarization. Cross and circle points correspond to experimental data of x - and y -polarization, and dashed lines correspond to curve-fitting results.

By applying a super-cell method [12], we can calculate the propagation constants of the two modes at different temperatures. Although the temperature-induced cross-sectional change was intuitively regarded as small, simulation results shown in Fig. 4 illustrate that its influence over the propagation constant difference $\Delta\beta$ should be taken into consideration. However, in both cases, the differential propagation constant $\Delta\beta$ was found to vary linearly with the temperature, which can be conveniently used to evaluate the first part of (2) by calculating the slope of the curve.

Fig. 5 shows the theoretically calculated temperature sensitivity as a function of wavelength. Unlike the elliptical-core TM fiber [1], whose temperature sensitivity has a monotonic dependence on wavelength, the sensitivity of TM PCF has negative values and a parabolic-like relation with respect to the operating wavelength. The theoretical sensitivities agree in trends with the

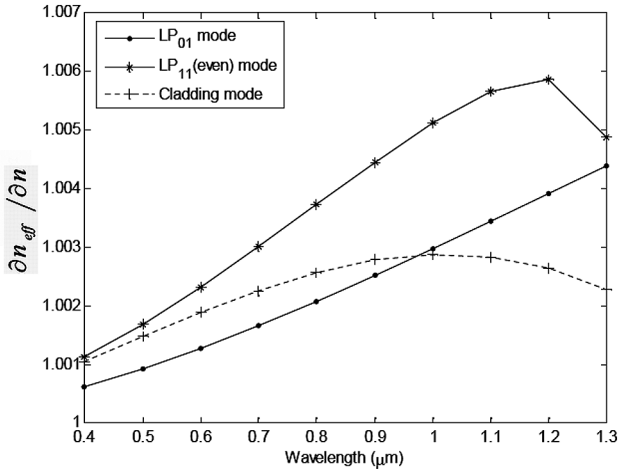


Fig. 6. $\partial n_{\text{eff}}/\partial n$ as a function of wavelength for LP_{01} , LP_{11} (even) and cladding mode.

experimentally measured results. The discrepancy between the measured and calculated values may be attributed to the idealized fiber structure and the residual thermal stress that is not considered during theoretical modeling. The real PCF has non-circular holes and nonuniform hole distribution (Fig. 1), and this will lead to difference between the estimated values from idealized model and experimental results. The asymmetrical nature of the PCF means that the thermal induced stress is not uniform across the fiber profile and it is difficult to quantitatively incorporate its contribution into the theoretical model for the practical PCF.

To understand the nonmonotonic dependence of temperature sensitivity on the operating wavelength, further theoretical investigation was conducted. First, simulation indicated the overall temperature sensitivity is dominated by the thermo-optic effect, which is at least an order of magnitude higher than the effects of fiber elongation ($\sim 3 \times 10^{-3}$) and transverse cross section expansion ($\sim 4 \times 10^{-2}$). We thus neglect the latter two factors and concentrate on the thermo-optical effect on the propagation constants. The sensitivity can now be rewritten as

$$\eta' = \frac{\partial(\Delta\beta)}{\partial T} = \frac{\partial(\Delta\beta)}{\partial n} \cdot \frac{\partial n}{\partial T} = n\kappa \cdot \frac{\partial(\Delta\beta)}{\partial n} \quad (4)$$

substituting $\Delta\beta = (2\pi/\lambda)(n_{\text{eff}}^{01} - n_{\text{eff}}^{11})$ to (4), where n_{eff}^{01} and n_{eff}^{11} are the effective index of the LP_{01} and LP_{11} (even) mode, respectively. The temperature sensitivity can be written as

$$\eta' = n\kappa \cdot \frac{\partial(\Delta\beta)}{\partial n} = n\kappa \cdot \frac{2\pi}{\lambda} \cdot \left(\frac{\partial n_{\text{eff}}^{01}}{\partial n} - \frac{\partial n_{\text{eff}}^{11}}{\partial n} \right) \quad (5)$$

where $\partial n_{\text{eff}}^{01}/\partial n$ and $\partial n_{\text{eff}}^{11}/\partial n$ is the rate of change of the effective index of the LP_{01} and LP_{11} (even) mode with respect to the background refractive index of silica, which has been shown in Fig. 6. For the LP_{01} mode $\partial n_{\text{eff}}^{01}/\partial n$ shows a linear relationship

with respect to the operating wavelength. However, $\partial n_{\text{eff}}^{11}/\partial n$ of the LP_{11} (even) mode shows a parabolic-like relationship with respect to the operating wavelength when the wavelength is approaching the cutoff wavelength ($\sim 1.32 \mu\text{m}$). The difference between $\partial n_{\text{eff}}^{01}/\partial n$ and $\partial n_{\text{eff}}^{11}/\partial n$, and hence, the overall temperature sensitivity as determined by (5) has a nonmonotonic dependence on wavelength. This agrees with the theoretical and experimental results as shown in Fig. 5.

IV. CONCLUSION

The temperature sensitivity of a TM PCF interferometric sensor was measured and it showed a nonmonotonic dependence on the operating wavelength. We present a theoretical analysis of the nonmonotonic wavelength response. The theoretical sensitivities agree in trends with the experimentally measured results. The unique temperature sensitivities of the TM Hi-Bi PCF described in this letter, coupled with the strain sensitivities presented in [9] can be used to perform temperature insensitive strain measurement [13].

REFERENCES

- [1] S. Y. Huang, J. N. Blake, and B. Y. Kim, "Perturbation effects on mode propagation in highly elliptical core two-mode fibers," *J. Lightw. Technol.*, vol. 8, no. 1, pp. 23–33, Jan. 1990.
- [2] B. Y. Kim, J. N. Blake, H. E. Engan, and H. J. Shaw, "All-fiber acousto-optic frequency shifter," *Opt. Lett.*, vol. 11, pp. 389–391, 1986.
- [3] D. Ostling and H. E. Engan, "Narrow-band acousto-optic tunable filtering in a two-mode fiber," *Opt. Lett.*, vol. 20, pp. 1247–1249, 1995.
- [4] H. S. Park, S. H. Yun, I. K. Hwang, S. B. Lee, and B. Y. Kim, "All-fiber add-drop wavelength-division multiplexer based on intermodal coupling," *IEEE Photon. Technol. Lett.*, vol. 13, no. 5, pp. 460–462, May 2001.
- [5] A. Ortigosa-Blanch, J. C. Knight, W. J. Wadsworth, J. Arriaga, B. J. Mangin, T. A. Birks, and P. St. J. Russell, "Highly birefringent photonic crystal fibers," *Opt. Lett.*, vol. 25, pp. 1325–1327, Sep. 2000.
- [6] K. Suzuki, H. Kubota, S. Kawanishi, M. Tanaka, and M. Fujita, "High-speed bi-directional polarization division multiplexed optical transmission in ultra low-loss (1.3 dB/km) polarization-maintaining photonic crystal fiber," *Electron. Lett.*, vol. 37, pp. 1399–1401, Nov. 2001.
- [7] T. P. Hansen, J. Broeng, S. E. B. Libori, E. Knuders, A. Bjarklev, J. R. Jensen, and H. Simonsen, "Highly birefringent index-guiding photonic crystal fibers," *IEEE Photon. Technol. Lett.*, vol. 13, no. 6, pp. 588–590, Jun. 2001.
- [8] W. Jin, Z. Wang, and J. Ju, "Two-mode photonic crystal fibers," *Opt. Express*, vol. 13, pp. 2082–2088, Mar. 21, 2005.
- [9] J. Ju, W. Jin, and M. S. Demokan, "Two-mode operation in highly birefringent photonic crystal fiber," *IEEE Photon. Technol. Lett.*, vol. 16, no. 11, pp. 2472–2474, Nov. 2004.
- [10] Q. Li, C. H. Lin, P. Y. Tseng, and H. P. Lee, "Demonstration of high extinction ratio modal interference in a two-mode fiber and its applications for all-fiber comb filter and high-temperature sensor," *Opt. Commun.*, vol. 250, pp. 280–285, 2005.
- [11] G. Statkiewicz, T. Martynkien, and W. Urbanczyk, "Measurements of modal birefringence and polarimetric sensitivity of the birefringent holey fiber to hydrostatic pressure and strain," *Opt. Commun.*, vol. 241, pp. 339–348, 2004.
- [12] Z. Wang, G. Ren, S. Lou, and W. Liang, "Investigation of the supercell based orthogonal basis function method for different kinds of fibers," *Opt. Fiber Technol.*, vol. 10, pp. 296–311, 2004.
- [13] W. Jin, W. C. Michie, G. Thursby, M. Konstantaki, and B. Culshaw, "Simultaneous measurement of strain and temperature: error analysis," *Opt. Eng.*, vol. 36, pp. 598–609, 1997.